

ELASTOGRAPHY: ELASTICITY IMAGING USING ULTRASOUND
WITH APPLICATION TO MUSCLE AND BREAST *IN VIVO*

I. Céspedes, J. Ophir¹, H. Ponnekanti and N. Maklad

Ultrasonics Laboratory, Department of Radiology
The University of Texas Medical School
Houston, TX 77030

Changes in tissue elasticity are generally correlated with its pathological state. In many cases, despite the difference in elasticity, the small size of a lesion or its location deep in the body preclude its detection by palpation. In general, such a lesion may or may not possess echogenic properties that would make it ultrasonically detectable. Elastography is an ultrasonic method for imaging the elasticity of compliant tissues. The method estimates the local longitudinal strain of tissue elements by ultrasonically assessing the one dimensional local displacements. This information can be combined with first order theoretical estimates of the local stress to yield a quantitative measure of the local elastic properties of tissue. The elasticity information is displayed in the form of a gray scale image called an elastogram. An experimental system for elastography in phantoms based on a single element transducer has been described previously [1]. Here we introduce a new elastography system based on a linear array transducer that is suitable for *in vivo* scanning. We describe tissue mimicking phantom experiments and preliminary *in vivo* breast and muscle elastograms confirming the feasibility of performing elastography *in vivo*. An elastogram of a breast containing an 8 mm palpable cancer nodule clearly shows the lesion. Elastograms and their corresponding sonograms show some similarities and differences in the depiction of tissue structures. © 1993

Academic Press, Inc.

Key words: Breast; elasticity; elastography; muscle; ultrasound.

INTRODUCTION

Palpation is widely used today as a screening procedure for diseases of the breast, thyroid, prostate, and liver, since pathological changes in tissue are generally correlated with elasticity changes as well. Measurements of the elastic properties of tissue reported in the past resulted in a wide range of values [2,3], but no quantitative information is available on the elastic properties of tissues in normal and pathological breast, prostate, and other organs (except for a few *in vitro* prostate and liver measurements in [3]). Qualitative description of the hardness of pathological tissues can be found in the medical literature. Malignant lesions

¹Author to whom correspondence should be addressed.

generally present as hard nodules, e.g., scirrhous carcinoma of the breast, liver metastases, prostatic carcinoma, and thyroid cancer [4]. Scirrhous carcinoma of the breast, which is the most common cancer of the breast and constitutes about three fourths of all breast cancers, has been described as stony hard, but other types of breast cancers (e.g., intraductal and papillary carcinoma) are soft [5]. In many cases, despite the difference in elasticity, the small size of a pathological lesion or its location deep in the body preclude its detection and evaluation by palpation. For example, solid masses in the breast may or may not possess echogenic properties that would make it ultrasonically detectable [6], yet be much harder than the embedding tissue. Diffuse organ diseases may involve fatty and/or collagenous deposits that increase or decrease tissue elasticity. Diffuse diseases such as cirrhosis of the liver are known to significantly reduce the elasticity of the liver tissue as a whole [4], yet they may appear normal in conventional ultrasound examinations. In general, the echogenicity and the elasticity of tissue are uncorrelated.

Several ultrasonic methods for deriving information related to the elastic properties of soft tissues have been described in the past ten years. These have already been reviewed in a previous paper [1]. In [1], these techniques are classified based on the basic method of measurement of motion.

- a) Visual inspection techniques [7-9]. These are based on the visual examination of the ultrasound information to quantify the motion of tissue.
- b) Doppler based techniques [10-14], which generally consist of measurement of the velocity of propagation of a low frequency (10 Hz to 1 KHz) mechanical wave. This measurement is used to estimate tissue hardness through the relationship between the modulus of elasticity and the velocity of propagation, density, and frequency of the mechanical wave. Thus, Doppler based techniques make indirect assessment of tissue elasticity.
- c) Correlation based techniques [1, 15-21, 23-24]. These methods make direct estimation of tissue hardness by estimating the strain through measurements of local tissue displacement. The correlation based techniques may be classified further as depending on internal [15-19] or external [1, 20-21, 23-24] sources of mechanical excitation. The external sources of mechanical excitation may be classified as vibratory [20-21] or static [1, 23-24].

Elastography has been shown to be capable of imaging the local elasticity in phantom experiments [1, 22-27]. When a tissue volume is mechanically excited with a quasi-static compression, the internal stresses are defined by the boundary conditions as well as by the structure and properties of the tissue. In order to fully characterize the local elastic properties of the tissue volume, it is necessary to measure the stress and the resulting strain components in three orthogonal spatial directions (in the context of an ultrasound system, we may choose the axial, lateral and the elevational directions relative to the ultrasonic beam). However, when using conventional one dimensional array ultrasound transducers to estimate small strains (less than 2 %), two important limitations arise. First, an obvious but fundamental limitation is that the estimation of strain (or other parameters such as ultrasound backscatter) is confined to the ultrasonic scan plane. Second, the lateral resolution of the ultrasound system is poor compared to the magnitude of the expected lateral tissue displacements.² Therefore, a single linear array ultrasound system can be used to accurately measure small strains exclusively along the direction of the ultrasound beam. If the linear array (alone or as part of a larger

²This is due to the following: 1) the lateral resolution is typically several times worse than the axial resolution; 2) the lateral (shear) strain is at most one half of the longitudinal strain (for a Poisson's ratio of 0.5 the lateral strain is one half of the longitudinal strain); and 3) to minimize rf signal distortion the magnitude of the applied mechanical compression is regulated so as to result in axial displacements just within the axial detection capabilities of the system. For these reasons, the lateral displacement of tissues in elastography is typically small and practically undetectable.

compressor) is used to apply a small compression to the tissue, only the longitudinal strain can be estimated with any reasonable accuracy. However, it is possible, in principle, to use a set of orthogonal interrogating ultrasonic beams to assess displacement accurately in multiple directions [15]. This more complicated multiple transducer scheme is out of the scope of our current work.

In elastography, the ultrasound transducer is generally used to compress the tissue. The imparted compression is typically about 1% or less of the total depth of the tissue under investigation. Such small compressions are required in order to minimize the distortion of the signal due to the compression, and thus facilitate accurate time delay analysis. The local longitudinal strain information combined with local longitudinal stress information in the tissue can be used to generate quantitative images (elastograms) of local estimates of the elastic modulus. These local estimates are displayed in the form of an 8 bit gray scale image, where white represents softer tissues, black represents harder tissues, and the gray levels represent intermediate elasticities. Although elastography is an ultrasonic technique, the elastograms display elasticity information, not echo amplitude information as do conventional sonograms. The appearance of elastograms is therefore quite different from sonograms.

Elastograms exhibit reasonable spatial and parametric resolution in phantom studies. We have shown that 5 dB differences in elasticity can be easily detected in a phantom composed of synthetic foam layers with different elasticities [1]. In another phantom, we have also shown that small hard inclusions on the order of 3 mm in diameter embedded in a softer medium can be easily detected [2]. Nonmedical applications of elastography have been proposed, such as the use of elastography for the assessment of beef tenderness or the presence of fat [27]. We have described methods to improve the elastographic image quality based on simulations of targets of known elasticity [25]. The sensitivity, resolution, and contrast-to-noise ratio of elastography are currently being investigated.

In Ophir et al [1], we described an experimental system for performing elastography in phantoms based on a single element transducer. In that system, an image was formed with data obtained by sequential ultrasonic interrogation of adjacent lines of sight in the scan plane. However, this system was slow and hence not suitable for *in vivo* examinations. We also proposed to construct an *in vivo* elastography scanner using transducer array technology, which we have achieved recently. Hence, the objective of this paper is twofold: 1) to report on the new system suitable for performing elastography *in vivo* (and *in vitro*), utilizing a modified commercially available ultrasound scanner equipped with a linear array transducer; and 2) to investigate the feasibility of obtaining elastograms *in vivo*.

The new system was used to obtain elastograms and sonograms from healthy volunteers and a breast cancer patient. The breast was chosen as a target organ because of its clinical significance, its accessibility, and our goal of visualizing focal lesions using elastography. In addition, the calf muscle group was imaged, aiming at the visualization of muscle structure. To illustrate some of the properties of elastography, we also include two phantom experiments. The seam phantom contains a thin, soft, and isoechoic diagonal seam in a tissue mimicking synthetic foam. A second phantom consists of a piece of excised hard breast cancer tissue (of nonspecific etiology) embedded in a softer, nearly isoechoic gelatin phantom.

ELASTOGRAPHY

The basic elastography method has been described previously [1, 23-26]. A brief discussion of the basic principles of the method is presented here. When tissue is compressed

by a quasi-static stress, all points in the tissue experience a resulting level of three dimensional strain. Although tissue exhibits viscoelastic properties, we observe the elastic properties only since we apply a rapid compression. The slow viscous properties are ignored. In elastography, we apply a static stress from one direction, and concentrate on the estimation of strain along the ultrasound beam (longitudinal strain) in small tissue elements. If one or more of the tissue elements has a different hardness than the others, the level of strain in that element will be higher or lower and a harder tissue element will experience less strain than a softer one. The longitudinal component of the strain is estimated from the estimation of displacement from time shift measurements by assuming a constant speed of sound (1540 m/s). This is accomplished by: 1) acquiring a set of digitized rf A-lines from a region of interest in the tissue; 2) compressing the tissue (usually with the ultrasonic transducer) along the ultrasonic radiation axis by 1% (or less); 3) acquiring a second postcompression set of A-lines from the same region of interest in the tissue; and 4) performing crosscorrelation estimates of time shifts. Congruent A-lines are windowed into temporal segments and the corresponding time shifts of the segments are measured using correlation analysis. Accurate estimates of times shift were obtained using the correlation coefficient function (a normalized crosscorrelation function) [15, 17, 28, 20] in combination with quadratic peak interpolation [29-30]. The change in arrival time of the echoes in the segment before and after compression can thus be estimated. Due to the small magnitude of the applied compression there are only small distortions of the A-lines, and the resulting changes in arrival times are also very small (typically on the order of a few nanoseconds). The local longitudinal strain at the depth given by the product $i \times (\Delta T \times c \times 2)$, where c is the assumed speed of sound in the elastic medium, is calculated as

$$s(i) = \frac{\Delta t(i) - \Delta t(i-1)}{\Delta T} \quad (1)$$

where $\Delta t(i)$ is the time shift between segments in the indexed segment pair, and ΔT is the spacing between segments. The window is translated along the temporal axis of the A-line, and the calculation is repeated for all depths.

It has been noted in [1] that strain is a relative measure of elasticity since it depends on the magnitude of the applied compression as well as on the elastic composition of the material. Ultimately, it may be useful to obtain an absolute measure of the local elasticity in the tissue. Since we estimate one dimensional compression of tissue elements, the parameter of interest is the elastic modulus, or Young's modulus. In a uniform isotropic medium under uniaxial stress, the elastic modulus (E) is defined as

$$E = \frac{\sigma}{s},$$

where s and σ are the strain and the stress [31]. Elastograms are basically strain images. To obtain calibrated elastograms, we normalize the strain estimates by the estimated local stress. Under the assumption of tissue uniformity, isotropy, and uniaxial longitudinal stress, such calibrated elastograms are images of the inverse elastic modulus. Deviations from these assumptions result in corresponding deviations of the imaged parameter from the true inverse elastic modulus. Note that we have chosen to image the inverse elastic modulus, and not the

elastic modulus directly, for image consistency between calibrated and uncalibrated elastograms.

The internal stress is defined by the boundary conditions and by the structure of the tissue. Therefore, *a priori* estimation of the exact stress field is impossible, since it is target dependent. However, theoretical estimates of the stress distribution due to the external boundary conditions can be obtained [26]. In practice, when the compression is applied with a compressor that is large compared to the dimension of the tissue volume under examination, the stress in the tissue is approximately uniform and uniaxial, with a slight magnitude decay with depth [26]. Previous experiments show that if the width and the depth of the region of interest are close to the dimensions of the compressor, the stress variations due to external boundary conditions is small [22]. In this paper, we have assumed uniform longitudinal stress and therefore the elastograms were not calibrated and simply display strain estimates. The gray scale on the images is linear between 0% (black) and 2% (white) strain. Strain estimation becomes unreliable due to rf signal distortion at strains larger than 2%.

METHOD AND MATERIALS

The elastography system consists of a Diasonics Spectra II ultrasound scanner (Diasonics Inc., Milpitas, CA) equipped with a 5 MHz linear array, a Lecroy 8 bit digitizer (Lecroy Corp., Spring Valley, NY) operating at 50 MHz, a motion control system, a compression device, and a personal computer which controls the operation of the system (Fig. 1). The compression device consists of a CGR-600 X-ray mammography paddle (GE/CGR,



Fig. 1 Clinical setup of the elastography system in the clinical mammography room.

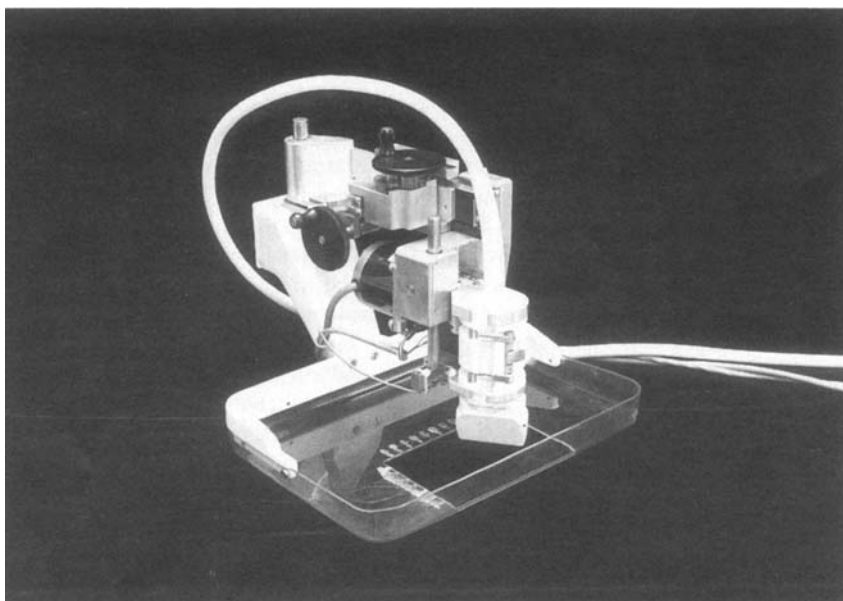


Fig. 2 Positioning device for elastography. The positioning device allows three-dimensional motion and rotation of the transducer. The vertical compressional motion is mechanically operated under computer control. Lateral motion is manual. The transducer makes acoustic contact with the skin through a 6 cm by 11 cm opening in the compression paddle. The opening is marked with a coordinate system for mammographic localization of potential lesions.

Milwaukee, WI) that was modified to accommodate a transducer holder and a positioning device (Fig. 2). The objective of the mammography paddle is twofold: 1) in general, the paddle can be used to hold the tissue in position, since it is important in elastography to minimize sources of motion other than the applied compression; and 2) for breast studies, the elastography system can be used in conjunction with X-ray mammography. In this case, the transducer positioning device can be moved out of the way for the acquisition of the mammogram. The use of mammographic localization for ultrasound evaluation has been proposed in the past [32]. The positioning device allows 3 dimensional motion and rotation of the transducer around its axis. Transducer motion along the length of the window in the paddle was provided using a crank handle connected to a worm gear and rack arrangement. Each turn of the crank handle produced a 4 mm travel of the transducer. Motion across the window was provided by another crank handle coupled to a rack and pinion arrangement with a gearing ratio producing 4 mm of travel per turn. In addition, both these degrees of freedom were provided with levers for quickly disengaging the gears for easy removal of the mechanism from the path for obtaining a mammogram. Motion in the vertical direction is driven by a dc step motor with 65 oz-in peak torque and 25000 steps/rev, through a rack and pinion arrangement with a 5:1 gearing ratio. Motion was provided via a driver/controller unit (SX6, Compumotor, Rohnert Park, CA) that communicates with the computer through an RS-232 interface. Limit switches are located at the ends of the vertical travel. A remote toggle arrangement was also provided for easy initial positioning of the transducer. The

transducer makes acoustic contact with the skin through a 6 cm by 11 cm opening in the compression paddle. The opening is marked with a coordinate system for lesion localization with mammography.

The elastographic procedure consists of the acquisition of pre- and post-compression rf frames and subsequent cross-correlation processing of such data. In a typical sequence of operation, the compression paddle first compresses the tissue to immobilize it. In the case of breast studies, the positioning device is moved out of the way to obtain the reference mammogram and then returned to its position. The transducer makes contact with the tissue through the mentioned opening, and is moved laterally within the window in order to locate a region of interest. Then, the computer instructs the scanner to obtain an rf frame (100 A-lines) for a specified tissue depth. The rf signals are digitized at 50 MHz (8 bits) under computer control. After an rf frame has been digitized, the computer moves the transducer towards the tissue, compressing it by a specified amount (typically 1% or less of the total tissue depth), and a second postcompression rf frame is acquired. Human subjects are asked to hold their breath during the scan to minimize motion due to respiration. The only desirable source of motion is the imparted compression as any other motion may degrade the quality of the elastogram. For this reason, the two frame acquisitions together with the corresponding compression are performed in a short time (typically less than 500 ms). The pre- and postcompression frames are then passed on to the processing program that produces the elastogram. The correlation processing has already been described elsewhere [1, 25]. In all experiments, the echo signals from the precompression frame are used to obtain a sonogram.

We have constructed two phantoms to demonstrate some of the properties of elastography. The slash seam phantom is made of open cell polyester foam (pore size of approximately 2 mm) and consists of two nearly identical triangular pieces obtained by diagonally cutting a foam block (12 cm by 12 cm by 14 cm) and then tightly rejoining the cut pieces. This resulted in a soft and isoechoic seam between 2 mm and 4 mm wide due to the broken pores in the region of the cut. The phantom was submerged in a small water tank at room temperature. The breast cancer phantom is an 8% gelatin phantom that contains a piece of excised breast cancer tissue (figure 4). The irregular piece of cancer tissue (approximately 3 cm by 2.5 cm by 3 cm) was located in the center of a gelatin cylinder 10 cm tall and 9 cm in diameter. At this concentration of gelatin, the elasticity of the gel phantom has been measured independently to be 28 ± 5 KPa. Diatomaceous earth (1%) was added to the gelatin in order to produce ultrasonic scattering [33].

The *in vivo* experiments were conducted on healthy volunteers and on a volunteer breast cancer patient. The compression paddle was used to hold the tissue in position during scanning. A small precompression was applied with the transducer to ensure good mechanical contact with the tissue. We report on three cases as follows:

- 1) A transverse medio-lateral scan of the right leg of a 29 year old healthy male volunteer was obtained at about 10 cm distal to the knee joint. The elastogram corresponds to a 40 mm wide by 50 mm deep region of interest in the relaxed muscles, starting at 5 mm below the skin surface.
- 2) With a 42 year old healthy volunteer in the sitting position, the right breast was pre-compressed to a thickness of about 40 mm and a transverse craniocaudal elastogram was obtained from a section close to the chest wall. The elastogram corresponds to a 40 mm wide by 35 mm deep region of interest, starting at 5 mm below the skin surface. A 0.4 mm compression was applied.
- 3) The right breast of a 62 year old volunteer patient with a relatively small (8 mm) hard palpable mass histologically confirmed to be infiltrating ductal carcinoma (scirrhous

carcinoma), was imaged. The volunteer patient was in the sitting position. The lesion was first localized through a reference mammogram. Without moving the patient, the ultrasound probe was positioned on the lesion using a gel pad stand-off. The lesion was visible on the sonogram. A craniocaudal elastogram was obtained starting at the skin surface and including the entire breast. The total depth of the breast was 35 mm and 0.6 mm compression was applied.

RESULTS

The elastogram and the sonogram of the slash seam phantom are shown in figure 3. The soft seam is not visible on the sonogram since it is isoechoic with the surrounding material. The seam appears as a soft (bright) line in the corresponding elastogram and measures approximately 2.7 mm in width. Lateral motion between the two parts of this phantom is unlikely to occur due to the roughness of the interface between them. Any lateral motion would result in decorrelation of the rf and a decrease of the effective longitudinal strain applied to the phantom. This, however, is not observed on the elastogram. Figure 4 shows the sonogram and the elastogram of the breast cancer phantom. The cancer is visible as a hard (dark) area on the elastogram.

Figure 5 shows the elastogram and the corresponding sonogram of the transverse scan of the calf. The sonogram and elastogram present different depictions of the calf muscles structure. The elastogram shows soft (bright) layers consistent with the location of the fascia layers (F) between muscles (particularly between the Gastrocnemius (G) and the Soleus (S)

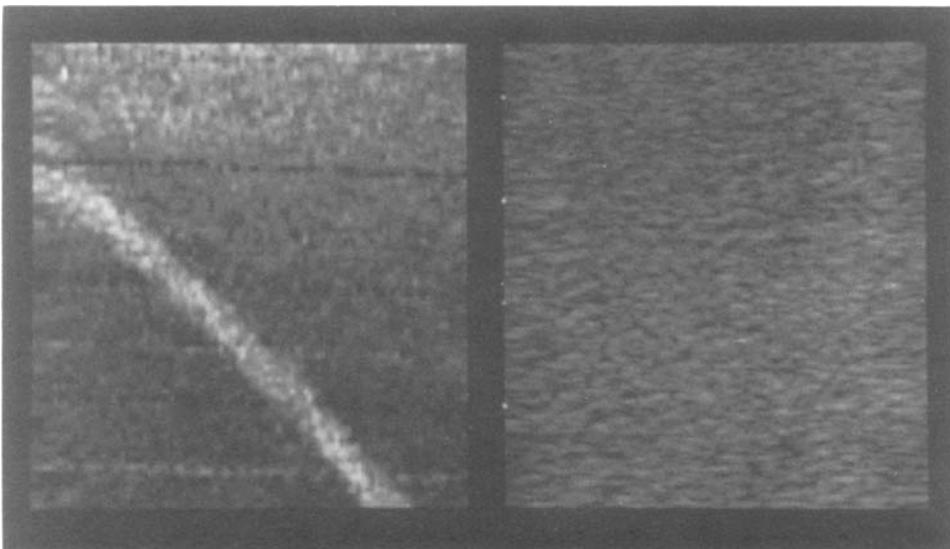


Fig. 3 Elastogram (left) and sonogram (right) of the slash seam foam phantom (width = 40 mm; depth = 45 mm). The soft seam appears bright (soft) on the elastogram and measures approximately 2.7 mm. The seam is invisible on the sonogram.

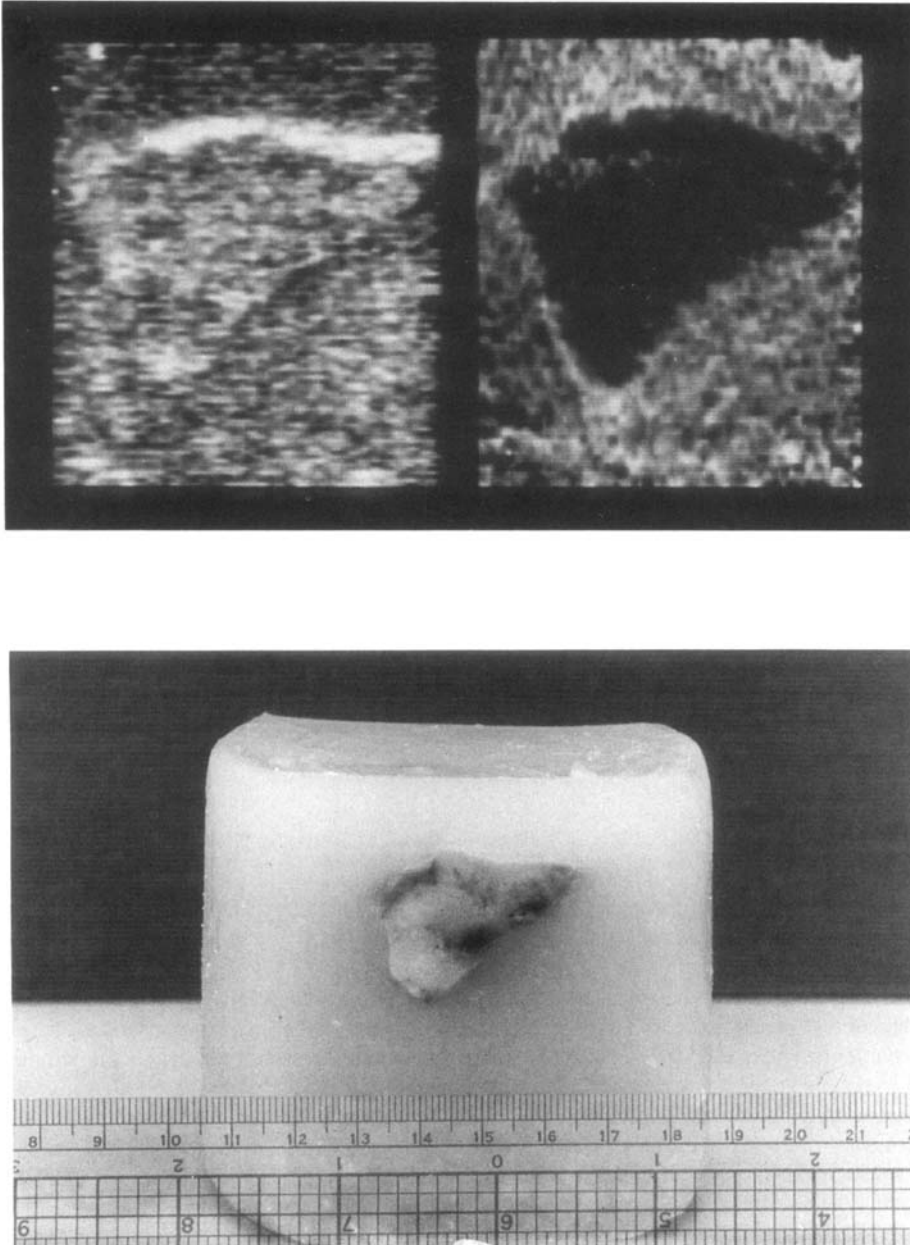


Fig. 4 Elastogram (right) and sonogram (left) of the breast cancer gel phantom (width = 40 mm; depth = 45 mm). The breast cancer tissue appears as a dark (black) area on the elastogram and it is also visible on the sonogram. The phantom was cut approximately through the scan plane of the elastogram (bottom).

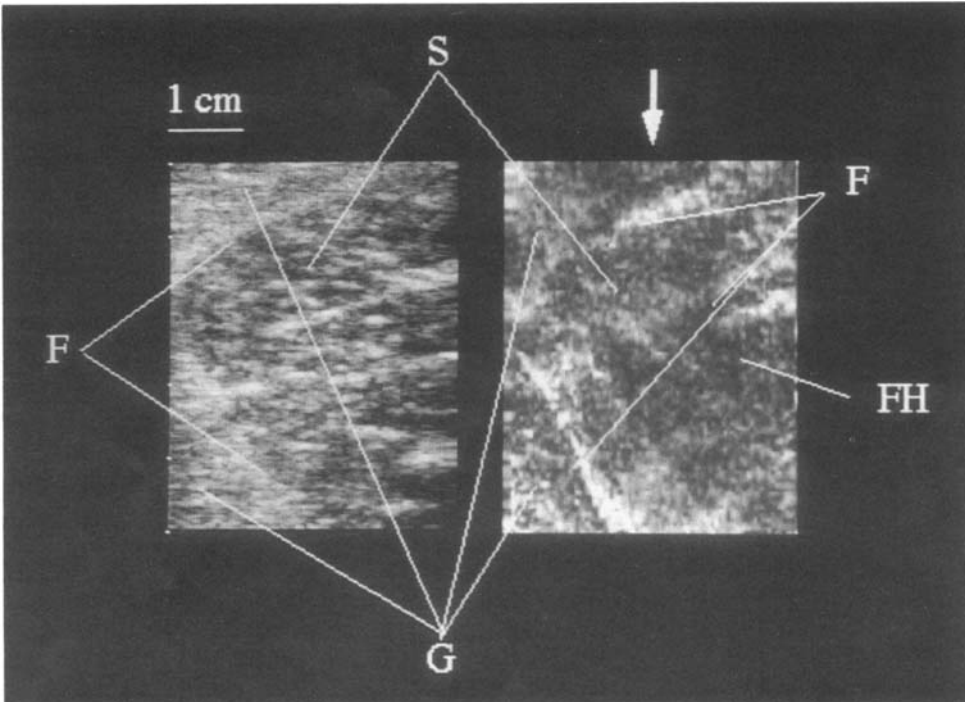


Fig. 5 Elastogram (right) and sonogram (left) of a transverse medio-lateral section of the calf muscles of a 29 year old healthy volunteer (width = 40 mm; depth = 50 mm). Observe fascia layers (F), particularly between the Gastrocnemius (G) and the Soleus (S) muscles, and the Flexor Hallucis Longus muscle (FH).

muscles; less evident between the Gastrocnemius and the Flexor Hallucis Longus (FH) and regions of higher and lower elasticity within the muscles) [34].

Figure 6 shows the transverse craniocaudal elastogram and sonogram from the breast representing a scanned area of approximately 40 mm wide by 35 mm deep. A good morphological correlation can be found among some structures appearing in the sonogram and in the elastogram. A range of elasticity values is demonstrated in the elastogram, which allows visual differentiation of tissue components. Adipose tissue appears as soft (light) in the elastogram. This is particularly evident in the subcutaneous fat layer proximally and distally to the transducer (SF), and in what appears to be a fatty band (FB) in the posterior half of the breast. These areas appear hypoechoic in the sonogram as expected. In some areas, structures consistent with the appearance of the lobular gland structure of the breast (LG) are shown in both sonogram and elastogram. However, while the glandular components appear hypoechoic in the sonogram (thus being indistinguishable from the adipose tissue), they appear as firm (dark) in the sonogram (unlike the adipose tissue). The elastogram is consistent with the known firmness of glandular tissue and the softness of adipose tissue. Overall, an organized, firm lobular structure (LG) can be clearly seen on the elastogram. This

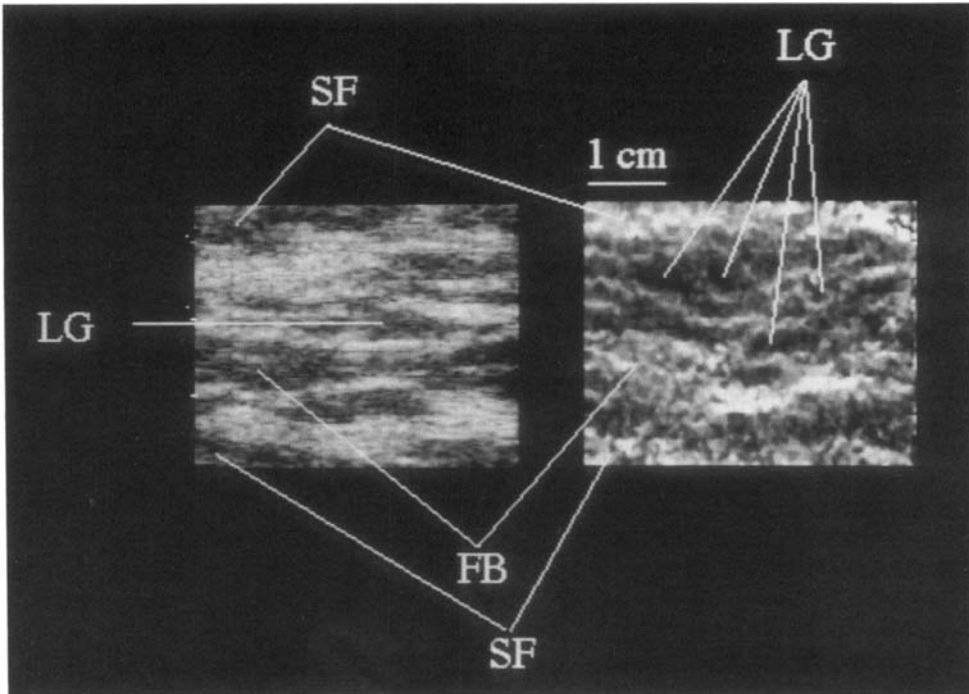


Fig. 6 Elastogram (right) and sonogram (left) of a transverse cranio-caudal section of the normal breast of a 42 year old healthy volunteer (width =40 mm; depth = 35 mm). Note the soft (light) subcutaneous fat (SF) along the front and back of the breast and the fatty band (FB) which appear hypoechoic on the sonogram. Structures consistent with the lobular gland structures (LG) can be observed in the elastogram, which correspond to glandular (heterogeneous) areas in the sonogram.

appearance is consistent with the normal anatomy of the breast, yet it cannot be seen on the sonogram.

Figure 7 shows the transverse craniocaudal elastogram and sonogram from the breast with the cancer representing a scanned area of approximately 40 mm wide by 35 mm deep. The mammogram shows a dense area (D) within the fatty tissue. In the elastogram, the cancer nodule (C) appears as a well delineated hard (black) area within the subcutaneous fatty area, which appears as soft (light). On the sonogram, the cancer (C) appears as a hyperechoic area with an relatively strong shadow. The cancer diameter measured on the elastogram is approximately 8 mm.

DISCUSSION AND CONCLUSIONS

We have successfully implemented an elastography scanner based on a linear array transducer. Using this system, we have shown the feasibility of *in vivo* elasticity imaging, thus extending our previous results in phantoms and tissues *in vitro* [1,22]. A 500 ms acquisition

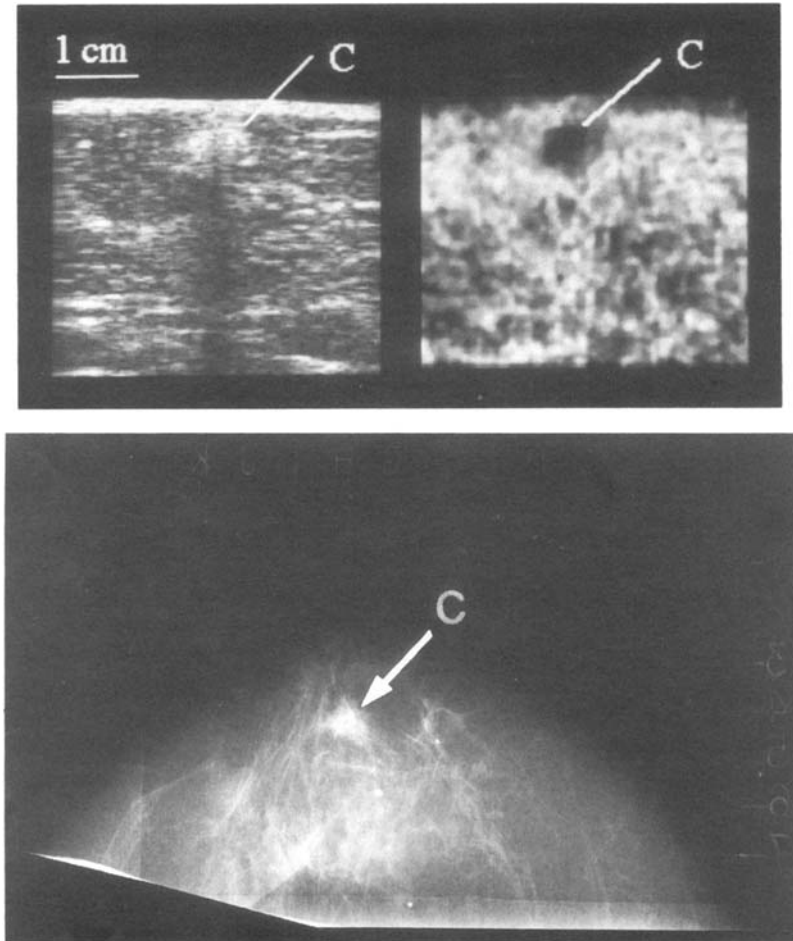


Fig. 7 Elastogram (right) and sonogram (left) of a transverse cranio-caudal section of the right breast of a 62 year old volunteer patient (width = 40 mm; depth = 35 mm). Mammogram of the right breast showing a dense area (bottom). The elastogram shows a well defined hard (black) area, approximately 8 mm in diameter, within the soft (white) fat. On the sonogram the cancer nodule appears as a hyperechoic area, followed by a relatively strong shadow behind it.

time appears adequate to avoid respiratory and arterial pulsating motion when scanning the limbs and the breast. Elastography has not been tested in other organs where paracardiac and respiratory motion may present a more fundamental problem. However, the acquisition time can be decreased further to approximately 100 ms, thus reducing the effect of undesired motion. Additionally, cardiac gating could also be used, since it can effectively reduce the effect of tissue motion [15]. The ultimate limits of the scanning time are set by the speed of sound in the body ($\approx 1540\text{m/s}$) and by the speed of propagation of the elastic wave generated by the applied compression (\approx tens of m/s) [10].

The slash seam phantom experiment shows that elastography is capable of imaging structures that are invisible on the sonogram, since each method depicts different properties, i.e., elasticity and backscatter. The soft seam is visible on the elastogram as a bright (soft) line, approximately 2.7 mm wide. The breast cancer phantom demonstrates a lesion that, while visible in the sonogram, is better defined in the elastogram. Note that the top margin of the cancer is approximately at normal incidence to the beam and therefore it is more evident on the sonogram than the other margins that are at an angle. In the elastogram, all interfaces are equally well defined. Judging by the strain ratio between the cancer and the gelatin, the Young's modulus of the cancer tissue is approximately 100 KPa.

The normal tissues of the calf and the breast demonstrate a high degree of elasticity contrast (approximately a 5 to 1 ratio), allowing visual differentiation of tissue components. The elasticity contrast was estimated from the elastograms by calculating the strain ratio of the hardest to the softest regions. The elastograms and corresponding sonograms show some similarities and many differences in the depiction of tissue structure, since they convey different information. In comparing sonograms and elastograms, good morphological registration of the image features is observed. The overall appearance of the elastogram is quite different from that of the corresponding sonogram. Elastograms do not exhibit sonographic speckle and present a smoother appearance. Currently, the noise (mean-to-standard deviation of the image) in elastograms of uniform tissues is less than half of that in sonograms. However, the noise level in elastograms can be reduced further with improved cross-correlation techniques [25].

The elastogram of the breast containing a scirrhous carcinoma nodule showed a well defined hard (black) area, approximately 8 mm in diameter, within the soft (white) fat. In this elastogram, we applied a relatively high strain which resulted in a noisy image (many strain estimates larger than 2%). For this reason, we have low-pass filtered the elastogram to achieve the normal elastographic appearance. The lesion is also visible in the mammogram. Sonographically, the cancer appears as a hyperechoic area, producing a relatively strong shadow behind it; the shape and size of the lesion cannot be well defined from the sonogram due to the shadow.

The preliminary *in vivo* results indicate that elastography is capable of imaging of elastic properties of tissue *in vivo* with reasonable resolution and thus allows visualization of new tissue information. This technique may be especially suited for the detection of small hard or soft focal lesions located deep in the tissue, which may be difficult to detect sonographically, by palpation, or by other modalities.

ACKNOWLEDGMENTS

The authors wish to acknowledge the collaboration of K. Erikson and T. Toedtman in the design and construction of the system, and the assistance of J. Johnson and D. Klepac in the production of the pictures. This work was supported in part by a grant from Diasonics Corporation, Milpitas, CA.

REFERENCES

- [1] Ophir J., Céspedes I., Ponnekanti H., Yazdi Y., and Li X., Elastography: a quantitative method for imaging the elasticity of biological tissues, *Ultrasonic Imaging* 13, 111-134 (1991).

- [2] Fung, Y.C., *Biomechanics. Mechanical Properties of Living Tissues* (Springer-Verlag, New York, 1981).
- [3] Parker K., Huang S., Musulin R., and Lerner R., Tissue response to mechanical vibrations for "sonoelasticity imaging", *Ultras. Med. Biol.* 3, 241-246 (1990).
- [4] Anderson, W.A.D., *Pathology* (The C.V.Mosby Co., St. Louis, 1953)
- [5] Ariel, I.M. and Cleary, J.B., *Breast Cancer Diagnosis and Treatment* (McGraw-Hill, New York, 1987).
- [6] Jackson, V.D., The role of US in breast imaging, *Radiology* 177, 305-311 (1990).
- [7] Gore, J.C., Leeman, S., Metreveli, C., Plessner, N.T. and Wilson, K., Dynamic autocorrelation analysis of A-scans in vivo, in *Ultrasonic Tissue Characterization II*, M. Linzer, ed., NBS Spec. Publ. 525, pp. 275-280 (U.S. Government Printing Office, Washington, DC, 1979).
- [8] Eisensher, A., Schweg-Toffler, E., Pelletier, G. and Jacquemard, G., La palpation échographique rythmée - échosismographie, *Journal de Radiologie* 64, 255-261 (1983).
- [9] Birnholz, J.C. and Farrell, E.E., Fetal lung development: compressibility as a measure of maturity, *Radiology* 157, 495-498 (1985).
- [10] Truong, X.T., Jarrett, S.R., and Nguyen, M.C., A method for deriving viscoelastic modulus for skeletal muscle from transient pulse propagation, *IEEE Trans. Biomed. Eng. BME-25*, 382-384 (1978).
- [11] Levinson, S.F., Ultrasound propagation in anisotropic soft tissues: the application of linear elastic theory, *J. Biomech.* 20, 251-260 (1987).
- [12] Krouskop, T.A., Dougherty, D.R. and Levinson, S.F., A pulsed doppler ultrasonic system for making noninvasive measurements of the mechanical properties of soft tissue, *J. Rehabil. Res. Dev.* 24, 1-8 (1987).
- [13] Lerner, R.M. and Parker, K.J., Sono-elasticity in Ultrasonic Tissue Characterization and Echographic Imaging, in *Proc. 7th Eur. Comm. Workshop*, J.M. Thijssen, ed., October 1987, Nijmegen, The Netherlands.
- [14] Yamakoshi, Y. and Sato, T., Ultrasonic imaging of internal vibration of soft tissue under forced vibration. *IEEE Trans. Ultrason. Ferroel. Freq. Control* 17, 45-53 (1990).
- [15] Dickinson, R.J. and Hill, C.R., Measurement of soft tissue using correlation between A-scans, *Ultrasound Med. Biol.* 8, 263-277 (1982).
- [16] Wilson, L.S. and Robinson, D.E., Ultrasonic measurement of small displacements and deformations of tissues, *Ultrasonic Imaging* 4, 71-82 (1982).

- [17] Tristram, M., Barbosa, D.C., Cosgrove, D.O., Nassiri, D.K., Bamber, J.C., and Hill, C.R., Ultrasonic study of in vivo kinetic characteristics of human tissues, *Ultrasound Med. Biol.* 12, 927-937 (1986).
- [18] Adler, R.S., Rubin, J.M., Bland, P.H. and Carson, P.L., Quantitative tissue motion analysis of digitized M-mode images: gestational differences of fetal lung. *Ultrasound Med. Biol.* 16, 561-569 (1990).
- [19] De Jong, P.G.M., Arts, T., Hoeks, A.P.G. and Renneman, R.S., Determination of tissue motion velocity by correlation interpolation of pulsed ultrasonic echo signals, *Ultrasonic Imaging* 12, 84-98 (1990).
- [20] Bohs, L.N. and Trahey, G.E., A novel method for angle independent ultrasonic imaging of blood flow and tissue motion, *IEEE Trans. Biomed. Eng. BME-38*, 280-286 (1991).
- [21] Yagi, S. and Nakayama, K., Local displacement analysis of inhomogeneous soft tissue by spatial correlation of RF echo signals, in *Proc. 1988 World WFUMB Meeting*, p. 133 (1988) (abstract).
- [22] Céspedes I. and Ophir J., Elastography, experimental results from phantoms and tissues, *Ultrasonic Imaging* 13, 187 (1991) (abstract).
- [23] Ophir J. and Yazdi Y., US Patent 5,107,837 (1992).
- [24] Ophir, J., Céspedes I., and Ponnekanti, H., US Patent 5,178,147 (1993).
- [25] Céspedes I., Ophir, J., and Ponnekanti, H., Reduction of image noise in elastography, *Ultrasonic Imaging*, this issue (1993).
- [26] Ponnekanti, H., Ophir, J., and Céspedes, I., Axial stress distributions between coaxial compressors in elastography: an analytical model, *Ultrasound Med. Biol.* 18, 667-673 (1992).
- [27] Ophir, J., Miller, R.K., Ponnekanti, H., Céspedes, I., and Whittaker, A.D., Elastography of Beef Muscle, in *Proc. 38th International Congress of Meat Science and Technology*, vol. 1, pp. 153-159 (1992).
- [28] Bendat, J.S. and Piersol, A.C., *Random Data: Analysis and Measurement*, 2nd Edition, Ch. 8, p. 170 (John Wiley and Sons, New York, 1986).
- [29] Boucher, R.E. and Hassab, J.C., Analysis of discrete implementation of the generalized cross-correlator, *IEEE Trans. Acoust, Speech, Sig. Proc. ASSP-29*, 609-611 (1981).
- [30] Foster, G.C., Embree, M.P. and O'Brien, W.D., Flow velocity profile via time-domain correlation: error analysis and computer simulation. *IEEE Trans. Ultrason Ferroel. Freq. Control* 37, 164-174 (1990).
- [31] Saada A., *Elasticity, Theory and Applications* (Pergamon Press, New York, 1974).

- [32] Conway, W.F., Hayes, C.W., and Brewer, W.H., Occult breast masses: Use of a mammographic localization grid for US evaluation, *Radiology* 181, 143-146 (1991).
- [33] Eggleton, R.C. and Whitcomb, J.A., Tissue Simulators for Diagnostic Ultrasound, in *Ultrasound Tissue Characterization II*, M. Linzer, ed., NBS Special Publ. 525, pp. 327-336, (U.S. Government Printing Office, Washington, DC, 1979).
- [34] Williams P.L., ed., *Gray's Anatomy*, 37th Edition, p. 646 (Churchill Livingstone, London, 1989).